Fluctuation-dissipation ratio for compacting granular media

Alain Barrat,[1] Vittoria Colizza,[2,3] and Vittorio Loreto[3]

[1]*Laboratoire de Physique Théorique, Unité Mixte de Recherche UMR 8627, Bâtiment 210, Université de Paris-Sud, 91405 Orsay Cedex, France*
[2]*International School for Advanced Studies (SISSA), via Beirut 4, 34014 Trieste, Italy*
[3]*Physics Department, "La Sapienza" University in Rome, Piazzale A. Moro 5, 00185 Rome, Italy
and INFM, Center for Statistical Mechanics and Complexity, Rome, Italy*

In this paper we investigate the possibility of a dynamical definition of an effective temperature for compacting granular media in the framework of the fluctuation-dissipation (FD) relations. We have studied two paradigmatic models for the compaction of granular media, which consider particles diffusing on a lattice, with either geometrical (tetris model) or dynamical (Kob-Andersen model) constraints. Idealized compaction without gravity has been implemented for the tetris model, and compaction with a preferential direction imposed by gravity has been studied for both models. In the ideal case of an homogeneous compaction, the obtained FD ratio is clearly shown to be in agreement with the prediction of Edwards' measure at various densities. Similar results are obtained with gravity only when the homogeneity of the bulk is imposed. In this case the FD ratio obtained dynamically for horizontal displacements and mobility and from Edwards' measure coincide. Finally, we propose experimental tests for the validity of the Edwards' construction through the comparison of various types of dynamical measurements.

PACS number(s): 45.70.Cc, 05.70.Ln, 05.20.−y

I. INTRODUCTION

Granular materials [1–3] play a very important role in many fields of human life and industrial activities, such as agriculture, building, chemistry, etc. Their properties are interesting not only for practical reasons, but also from the point of view of fundamental physics. In fact, in spite of their apparent simplicity, they display a wide variety of behaviors that is only partially understood in terms of general physical principles.

A. Typical problems to face in the study of compact granular matter

The common wisdom about granular materials defines them as nonthermal systems, since thermal energy can be generally neglected if compared to mechanical energy due to gravity and other external energy sources usually acting on these systems. In addition, a fundamental role in the dynamics is played by the mechanical energy dissipation due to friction and collisions among the grains and with the container walls: motion can take place only by continuously feeding energy into the system that otherwise would get stuck into some metastable state, no longer exploring spontaneously the configuration space. Consequently, as a matter of fact, the dynamics of granular matter is always a response to an external perturbation and in general the response will depend in a nontrivial way on the rheological properties of the medium, on the boundaries, on the driving procedure and, last but not the least, on the past history of the system.

From the nonthermal character of these systems a lot of consequences can be drawn. The first one concerns the lack of any ergodicity principles: a granular media is not able to freely explore its phase space and the dynamical equations do not leave the microcanonical or any other known en-

semble invariant. Moreover, just as in the case of aging glasses, the compaction dynamics [4–6] does not approach any stationary state on experimental time scales (at least at small enough forcing) and these systems exhibit aging [7–9] and memory [10–12]. A granular media lives then always in nonequilibrium conditions. Even when one observes some stationary state as the result of a specific dynamics (energy injection) imposed to the system, one is never able to establish some sort of equipartition principle ruling how the energy injected is redistributed among the different degrees of freedom of the system.

Despite all these difficulties, since granular systems involve a large number of particles, one is always naturally inclined to treat them with methods of statistical mechanics. In particular, one of the main questions concerns the very possibility to construct a coherent thermodynamics and on this point the debate is wide open. The construction of a thermodynamics would imply the identification of a suitable distribution that is left invariant by the dynamics (e.g. the microcanonical ensemble), and then the assumption that this distribution will be reached by the system, under suitable conditions of "ergodicity." As already mentioned since in granular media energy is lost through internal friction, and gained by a nonthermal source such as tapping or shearing, this approach seems doomed from the outset. Nevertheless, one could ask whether some elementary thermodynamic quantities are well defined and what is their meaning. It is in this spirit that in this paper we address the question of the definition of an effective temperature for compact granular media. Before going in the details let us briefly review the state of the art on these subjects.

B. State of the art

A lot of approaches [13–22] have been devised in the last years to provide a coherent scenario but till now the situation

is quite uncertain mainly because at a fundamental level there is no general argument showing that a particular construction should lead to the relevant distribution for the dynamics (as one does in the case of conservative dynamics, leading to thermodynamics).

Many models have been proposed in order to reproduce the rich phenomenology observed in granular compaction experiments [4,5], but a general thermodynamical-like framework, based on the idea of describing a granular material with a small number of parameters is, however, still lacking.

A very ambitious approach, aiming at such a description of dense granular matter has been put forward by Edwards and co-workers [18,19], by proposing an equivalent of the microcanonical ensemble: macroscopic quantities in a jammed situation should be obtained by a flat average over all *blocked configurations* (i.e., in which every grain is unable to move) of given volume, energy, etc. The strong assumption made here is that all blocked configurations are treated as equivalent and have the same weight in the measure.

Very recently, important progresses in this direction have been reported in various contexts: a tool to systematically construct Edwards' measure, defined as the set of blocked configurations of a given model, was proposed in Refs. [23,24]; it was used to show that the outcome of the aging dynamics of the Kob-Andersen (KA) [25] model (a kinetically constrained lattice-gas model) was correctly predicted by Edwards' measure. Moreover, the validity and relevance of Edwards' measure have been demonstrated [26] for the tetris model [21], for one-dimensional phenomenological models [27], for spin models with "tapping" dynamics [28], and for sheared hard spheres [29].

At present, however, the correspondence between Edwards' distribution and long-time dynamics is at best checked but does not follow from any principle. It is therefore important to continue to explore its range of validity and therefore to test its applicability to various kinds of models.

Another important message emerging from these studies concerns the link between Edwards' approach and the outcomes of the measurements of the fluctuation-dissipation relations. In Refs. [23,24,26] it has been shown in the framework of two non-mean-field models, the Kob-Andersen model and the tetris model, that the so-called Edwards' ratio (see below for its precise definition) coincides on a wide range of densities with the fluctuation-dissipation ratio (FDR) in homogeneous systems, i.e., in systems without any preferential direction. This paper extends those results providing a series of evidences for the validity of Edwards' approach in two main directions.

(i) First of all we focus on more realistic situations by considering the case of granular packings subject to gravity: this is an important example to test the role of large scale inhomogeneities, such as the density profiles along the preferential direction, whose treatment has to be performed very carefully in order to avoid apparently nonphysical results [30].

(ii) We present results concerning the independence of the FD ratio of the observables used for its definition.

It should be noted that previous measurements of FDR in the presence of gravity (and thus heterogeneities) have been attempted in Refs. [30,31]. However, the negative response functions observed in Ref. [30] was subsequently shown in Refs. [8,11] to be linked to memory effects [10], and not to Edwards' measure. Moreover, the measures of Refs. [30,31] were flawed by an incorrect definition of the correlation part of the fluctuation-dissipation ratio, due to the fact that one-time quantities are still evolving (see Sec. V for a detailed discussion). The conclusion of Ref. [31] about the existence of a dynamical temperature was thus premature.

The link established between Edwards' approach and the fluctuation-dissipation relations could open new perspectives from two different points of view. First of all from the experimental point of view where possibilities are open to (i) check the Edwards' measure by means of dynamical measurements; (ii) perform dynamical measurements (through the fluctuation-dissipation relations) of a "temperature" which should only depend on the density. This could allow for an at least partial equilibration of the disproportion existing between the huge number of theoretical/numerical works (and this paper contributes to this number) and the few experimental results. Moreover, very focused experimental results could help in discriminating between the different models proposed in literature. On the other hand, from the theoretical point of view one is left with several questions: why Edwards' measure seems to be correct in a wide range of situations? Is it possible to identify some first principles justifications or derivations for it? Why the outcomes of the Edwards' approach seem to coincide with the results of fluctuation-dissipation measurements?

This paper, far from being able to address all these questions, tries to make the link between Edwards' approach and the fluctuation-dissipation measurements firmer in several realistic situations and propose some possible experimental paths for its checking. The outline of the paper is as follows. We first recall in Sec. II the definition of the models under consideration, and in Sec. III how to construct Edwards' measure. The case of homogeneous compaction for the tetris model is described in Sec. IV, while fluctuation-dissipation ratios during a gravity-driven compaction are measured for both KA and tetris models in Sec. V. Finally, possible experiments are proposed in Sec. VI, and conclusions are drawn.

II. MODEL DEFINITION

The models we consider are lattice models, and in this sense are not realistic microscopic models of granular materials. However, they are worth investigating: on the one hand, they have been shown to reproduce the complex phenomenology of granular media (see Refs. [7,8,11,21] and Refs. [33,35]); on the other hand, the validity of Edwards' measure for some observables has already been shown in an ideal case of homogeneous compaction [23,24], making these finite-dimensional models good candidates for further investigations in more realistic situations, i.e., with heterogeneities induced by gravity and the existence of a preferential direction.

A. Tetris model

Under the denomination of "tetris" falls a class of lattice [21] models whose basic ingredient is the geometrical frustration. The models are defined on a two-dimensional square lattice with particles of randomly chosen shapes and sizes. The only constraint in the system is that particles cannot overlap: for two nearest-neighbor particles, the sum of the arms oriented along the bond connecting the two particles has to be smaller than the bond length. The interactions are hence not spatially quenched but determined in a self-consistent way by local particle configurations.

In the version we use (see Ref. [24]), the particles have a "T" shape (three arms of length $\frac{3}{4}d$, where d sets the bond size on the square lattice). The maximum density allowed is then $\rho_{max} = 2/3$.

B. Kob-Andersen model

The other model we consider is the so-called KA model [25], first studied in the context of mode-coupling theories [32] as a finite dimensional model exhibiting a divergence of the relaxation time at a finite value of the control parameter (here the density); this divergence is due to the presence in this model of the formation of "cages" around particles at high density (the model was indeed devised to reproduce the cage effect existing in supercooled liquids).

Though very schematic, it has then been shown to reproduce rather well several aspects of glasses [33], like the aging behavior with violation of FDT [34], and of granular compaction [35].

The successful comparison of aging dynamics and predictions of Edwards' measure was moreover shown for the first time for this model, in Refs. [23,24], in the idealized case of homogeneous compaction. On the other hand, a study of the violation of the FDT during the compaction process (under gravity) was undertaken in Ref. [31], and the existence of a dynamical temperature was advocated [45].

The model is defined as a lattice gas on a three-dimensional lattice, with at most one particle per site. The dynamical rule is as follows: a particle can move to a neighboring empty site, only if it has strictly less than ν neighbors in the initial and in the final position.

Following [25], we take $\nu = 5$: this ensures that the system is still ergodic at low densities, while displaying a sharp increase in relaxation times at a density well below 1. The dynamic rule guarantees that the equilibrium distribution is trivially simple since all the configurations of a given density are equally probable: the Hamiltonian is just 0 since no static interactions exist.

Moreover, it is also easy to consider a mixture of two types of particles, by considering particles of type 1 with a certain value ν_1 for the dynamical constraint, and particles of type 2 with $\nu_2 \neq \nu_1$ [35].

III. EDWARDS' MEASURE

Edwards' approach is based on a flat sampling over all the blocked configurations, i.e., configurations with all particles unable to move. This definition therefore depends on the model and the type of dynamics. For example, a particle is more easily blocked in presence of an imposed drift, e.g., gravity.

This approach, based on the idea of describing granular material with *a small number of parameters*, leads to the introduction of an entropy S_{Edw}, given by the logarithm of the number of blocked configurations of given volume, energy, etc., and its corresponding density $s_{Edw} \equiv S_{Edw}/N$. Associated with this entropy are the state variables such as "compactivity" $X_{Edw}^{-1} = (\partial/\partial V)S_{Edw}(V)$ and "temperature" $T_{Edw}^{-1} = (\partial/\partial E)S_{Edw}(E)$.

The explicit construction of Edwards' measure, as well as of the equilibrium measure, has been described in detail in Refs. [23,24] for the tetris and the KA models. In particular, Edwards' measure is obtained with an annealing procedure at fixed density. In order to select only the subset of configurations contributing to the Edwards' measure we introduce an auxiliary temperature T_{aux} (and the corresponding $\beta_{aux} = 1/T_{aux}$) and, associated with it, an auxiliary energy E_{aux} which, for each configuration, is equal to the number of mobile particles. A particle is defined as mobile if it can be moved according to the dynamic rules of the original model.

In particular, one measures $E_{aux}(\beta_{aux}, \rho)$, i.e., the decrease of the auxiliary energy at fixed density, performing an annealing procedure increasing progressively β_{aux}. From this measure one can compute the Edwards' entropy density defined by

$$s_{Edw}(\rho) \equiv s_{aux}(\beta_{aux} = \infty, \rho)$$

$$= s_{equil}(\rho) - \int_0^\infty e_{aux}(\beta_{aux}, \rho) d\beta_{aux}, \quad (1)$$

where $e_{aux}(\beta_{aux}, \rho)$ is the auxiliary Edwards' energy density and $s_{aux}(\beta_{aux} = 0, \rho) = s_{equil}(\rho)$ is the equilibrium entropy of the model.

For the KA model, the equilibrium entropy is simply the entropy of a lattice gas. It is worth, however, recalling that, for the tetris model (and in general when the equilibrium measure is not known analytically), the equilibrium measure can also be obtained with an annealing procedure: also in this case one introduces an auxiliary temperature $T'_{aux} = 1/\beta'_{aux}$ associated with an auxiliary energy E'_{aux} defined as the total particle overlaps existing in a certain configuration. For each value of T'_{aux} one allows the configurations with a probability given by $e^{(-\beta'_{aux}E'_{aux})}$. Starting with a large temperature T'_{aux} one samples the allowed configurations by progressively decreasing T'_{aux}. As T'_{aux} is reduced E'_{aux} decreases and only at $T'_{aux} = 0$ (no violation of constraints allowed) the auxiliary energy is precisely zero. The exploration of the configuration space can be performed working at constant density by interchanging the positions of couples of particles. This procedure is used to compute $E'_{aux}(\beta'_{aux}, \rho)$ and $e'_{aux}(\beta'_{aux}, \rho)$ (energy per particle), from which one can compute the equilibrium entropy per particle by the expression
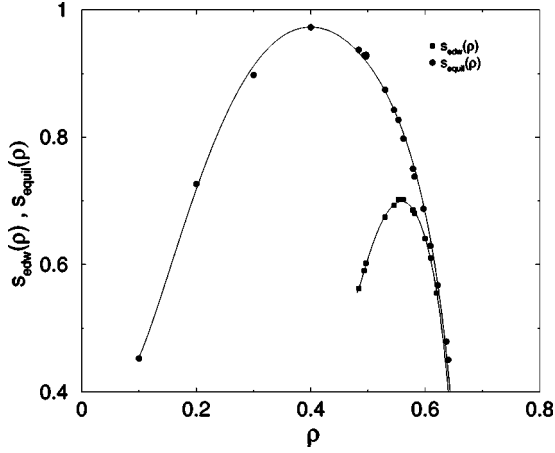
FIG. 1. $s_{Edw}(\rho)$ and $s_{equil}(\rho)$ for the tetris model.

$$s_{equil}(\rho) \equiv s_{equil}(\beta'_{aux} = \infty, \rho)$$

$$= s_{equil}(\beta'_{aux} = 0, \rho) - \int_0^\infty e'_{aux}(\beta'_{aux}, \rho) d\beta'_{aux},$$

where $e'_{aux}(\beta'_{aux}, \rho)$ is the auxiliary energy per particle. For the choice made for the particles one has

$$s_{equil}(\beta'_{aux} = 0, \rho) = -\rho \ln \rho - (1-\rho)\ln(1-\rho) + \rho \ln 4, \quad (2)$$

which is easily obtained by counting the number of ways in which one can arrange ρL^2 particles of four different types on L^2 sites.

Edwards' and equilibrium entropies, computed as a function of density, are reported in Fig. 1 for the tetris model. It is also possible to compute the so-called Edwards' ratio, defined as

$$X_{Edw} = \frac{ds_{Edw}(\rho)}{d\rho} \Big/ \frac{ds_{equil}(\rho)}{d\rho}. \quad (3)$$

X_{Edw} approaches 1 as $\rho \to \rho_{max}$, since at the maximum density all configurations become blocked and therefore equilibrium and Edwards' entropies become equivalent.

IV. FLUCTUATION-DISSIPATION RATIO FOR THE CASE WITHOUT GRAVITY

A. Tetris model: Dynamics without gravity

It is worth to recall that for the KA model, the compaction dynamics was obtained by means of a "piston," i.e. by creating and destroying particles only on the topmost layer (of a cubic lattice of linear size L) with a chemical potential μ [33]. The validity of Edwards' measure in this case has been described in Refs. [23,24]. We will therefore focus here on the tetris model. In Refs. [24,26], compaction dynamics without gravity has been implemented for this model in order to avoid generating a preferential direction.

The system is initialized through a random sequential adsorption of "T"-shaped particles on an initially empty lattice. The grains must satisfy the geometrical constraints with their nearest neighbors and cannot diffuse on the lattice. This filling procedure stops when no other particles can be deposited on the system anymore, yielding a reproducible initial density of $\rho \approx 0.547$.

The irreversible compaction dynamics is then realized alternating attempted random diffusions (in which a particle is chosen with uniform probability and allowed to move towards one of its nearest neighbors with probability $p = \frac{1}{4}$, only if all the possible geometrical constraints are satisfied) and attempted random depositions on the lattice (an empty site is chosen with uniform probability and a grain is then adsorbed on the lattice only if no violation of the geometrical constraints occurs). The global density increases, the system remaining homogeneous during the process.

The Monte Carlo (MC) time unit is defined as the number of elementary dynamical steps normalized to the number of sites of the lattice, L^2. In order to overcome the problem related to the simulation of very slow processes and obtaining a reasonable number of different realizations to produce clean data, we have devised a fast algorithm (in the spirit of Bortz-Kalos-Lebowitz algorithm [36]), where the essential ingredient is the updating of a list of mobile particles (whose number is n_{mob}). In order to reduce the number of less significant events, such as failed attempts of deposition/diffusion, this algorithm is essentially based on a guided dynamics where only mobile particles (i.e., grains that could diffuse toward a neighboring site) are considered. At each time step one *mobile* particle is chosen with uniform probability and allowed to move if all the geometrical constraints are satisfied. If the attempt has been successful, the list of mobile particles is then updated, performing a *local* control of grains' mobility. This procedure therefore introduces a temporal bias in the evolution of the system, which has to be taken into account by incrementing the time of an amount $\Delta t = 1/n_{mob}$, after each guided elementary step. This algorithm becomes very efficient as the density of the system increases, since the number of mobile particles reduces drastically.

During the compaction, we measure the density $\rho(t)$ of particles, the density $\rho_{mob}(t)$ of mobile particles, the mobility

$$\chi(t_w, t_w + t) = \frac{1}{dN} \sum_a \sum_{k=1}^N \frac{\delta\langle[r_k^a(t_w + t) - r_k^a(t_w)]\rangle}{\delta f}$$

obtained by the application of a random force to the particles between t_w and $t_w + t$, and the mean square displacement

$$B(t_w, t_w + t) = \frac{1}{dN} \sum_a \sum_{k=1}^N \langle[r_k^a(t_w + t) - r_k^a(t_w)]^2 \rangle$$

(N is the number of particles; $a = 1, \ldots, d$ runs over the spatial dimensions: $d = 2$ for tetris, $d = 3$ for KA; r_k^a is measured in units of the bond size d of the square lattice). Indeed, the quantities $\chi(t_w, t_w + t)$ and $B(t_w, t_w + t)$, at equilibrium, are linearly related (and actually depend only on t since time-translation invariance holds) by
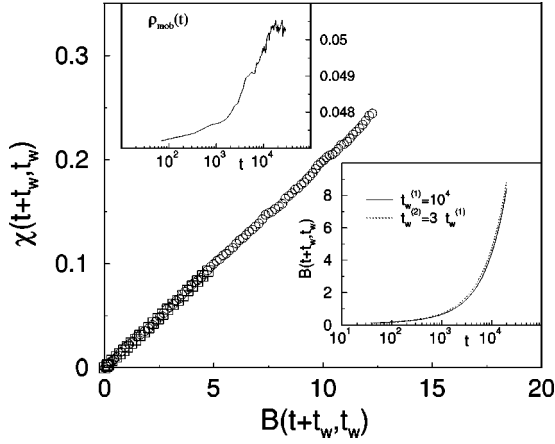
FIG. 2. Einstein relation in the tetris model with interrupted aging, at various densities. Insets, density of mobile particles vs t for $t_w = 10^4$, and $B(t_w+t, t_w)$ vs t for two different t_w (illustration of TTI).

$$2\chi(t) = \frac{X}{T_d^{eq}} B(t), \qquad (4)$$

where X is the so-called FDR which is unitary in equilibrium. Any deviations from this linear law signals a violation of the Fluctuation-Dissipation Theorem (FDT). Nevertheless, it has been shown, first in mean-field models [37], then in various numerical simulations of finite dimensional models [38,39] how in several aging systems violations from Eq. (4) reduce to the occurrence of two regimes: a quasiequilibrium regime with $X=1$ (and time-translation invariance) for "short" time separations ($t \ll t_w$), and the aging regime with a constant $X \le 1$ for large time separations. This second slope is typically referred to as a dynamical temperature $T_{dyn} \ge T_d^{eq}$ such that $X = X_{dyn} = T_d^{eq}/T_{dyn}$ [40].

We have simulated lattices of linear size $L = 50, 100, 200$, in order to ensure that finite-size effects were irrelevant. We have chosen periodic boundary conditions on the lattice, having checked that other types of boundary conditions (e.g., closed ones) gave the same results. We have investigated the irreversible compaction dynamics of the system up to times of 2×10^5 MC steps, realizing a large number of different runs ($N_{runs} \simeq 8000 - 9000$), in order to obtain clean data. The random perturbation is realized by varying the diffusion probability of each particle from the initial value $p = \frac{1}{4}$ to the value $p^\epsilon = \frac{1}{4} + f_i^r \epsilon$, where $f_i^r = \pm 1$ is a random variable associated with each grain independently for each possible direction ($r = x, y$), and ϵ represents the perturbation strength. The results presented here are obtained with a perturbation strength $\epsilon = 0.005$, having checked that for $0.002 < \epsilon < 0.01$ nonlinear effects are absent.

B. Interrupted aging regime

When the compaction process is stopped at a certain time t_w, the system relaxes towards equilibrium: the mean-square displacement and the integrated response function satisfy the TTI, as Fig. 2 shows. This is the so-called regime of inter-
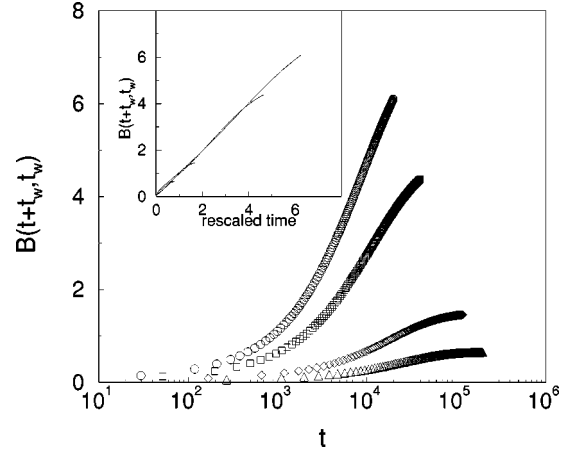

FIG. 3. Evolution of $B(t+t_w, t_w)$ for various t_w (from bottom to top, 5×10^3, 10^4, 3×10^4, and 5×10^4). Inset, collapse of B; for the collapse, we have not taken into account the final portion of each curve, because of a saturation of B due to finite-size effects.

rupted aging, characterized by an increase of $\rho_{mob}(t)$ toward its equilibrium value (inset of Fig. 2) and a single linear relation for the χ vs B parametric plot. Fluctuation-Dissipation Theorem is then recovered, and the value of the equilibrium fluctuation-dissipation ratio, T_d^{eq}, is obtained from the measures of those quantities; its value actually does not depend on the density of the system.

It is interesting to mention that the behavior described in this subsection can actually also be observed for the KA model, which was studied in Refs. [23,24] only under continuous compaction.

C. Aging dynamics

If the compaction is not stopped at time t_w, the density increases, and a typical aging behavior is observed, as shown in Fig. 3 where different curves of $B(t+t_w, t_w)$, for different values of t_w, are reported: the mean-square displacement depends explicitly not only on the observation time t but also on t_w. The system remains out of equilibrium on all the observed time scale, with the violation of TTI. The inset of Fig. 3 shows the collapse of the curves of $B(t+t_w, t_w)$ for different values of the age of the system, obtained with the following scaling function:

$$B(t+t_w, t_w) = c \left[\frac{\ln\left(\frac{t+t_w+t_s}{\tau}\right)}{\ln\left(\frac{t_w+t_s}{\tau}\right)} - 1 \right], \qquad (5)$$

where c, t_s, and τ are fit parameters. Our results show a linear dependence of the parameters t_s and τ on the age of the system, while the coefficient c is nearly constant.

Moreover, we observe the density of mobile particles $\rho_{mob}(t)$ getting smaller than the corresponding value at equilibrium [24], as another evidence of the out of equilibrium behavior of the system during the compaction process.

The system also features a violation of the fluctuation-dissipation theorem. More precisely, the χ vs B parametric
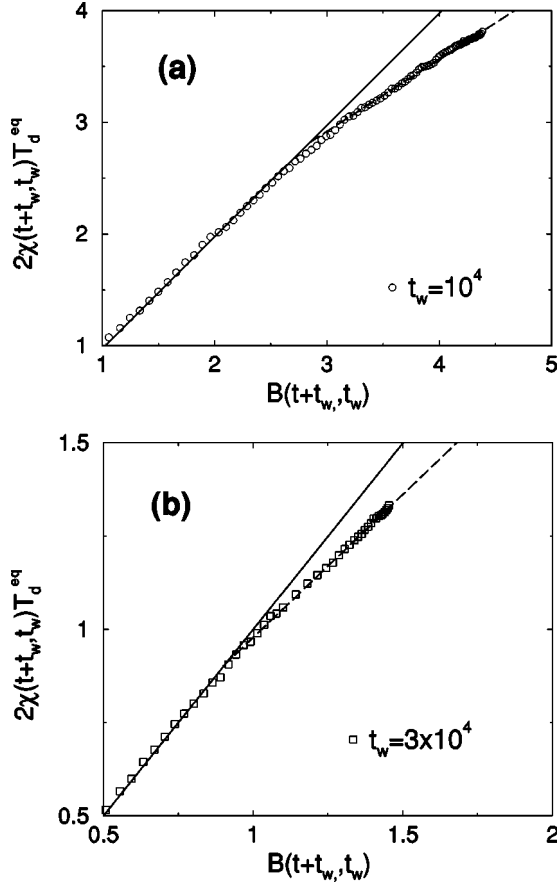
FIG. 4. Einstein relation in the tetris model: plot of the mobility $2T_d^{eq}\chi(t_w,t_w+t)$ vs the mean-square displacement $B(t_w,t_w+t)$ for (a) $t_w^1=10^4$ and (b) $t_w^2=3\times10^4$. The value of T_d^{eq} is taken from Fig. 2, and the slope of the full straight line is one. The dashed lines are linear of the FDT violation whose slope gives a measure of X_{dyn}.

plot, reported in Fig. 4, shows two different linear behaviors: for times t smaller than t_w we observe a first quasiequilibrium regime where FDT holds (i.e., $X_{dyn}=1$), followed by a second regime in which FDT breaks down and a dynamical temperature T_{dyn} arises which is independent of the observation time t. This quantity actually depends on the age of the system, t_w, and therefore on the density. We have investigated this behavior in a large range of waiting times, corresponding to several values of the density, obtaining the following results: $X_{dyn}^1=0.646\pm0.002$, $X_{dyn}^2=0.767\pm0.005$, $X_{dyn}^3=0.784\pm0.005$ at $t_w^1=10^4$, $t_w^2=3\times10^4$, and $t_w^3=5\times10^4$.

D. Results for a bidisperse system

In order to investigate the dependence of the dynamical temperature on the observables considered for its definition, we have introduced two different types of particles. Besides the "T"-shaped particles, already seen at the beginning of the section, we have considered "L"-shaped particles. Such grains are characterized by a different degree of disorder, so we expect these particles, the "smaller" ones, to move more
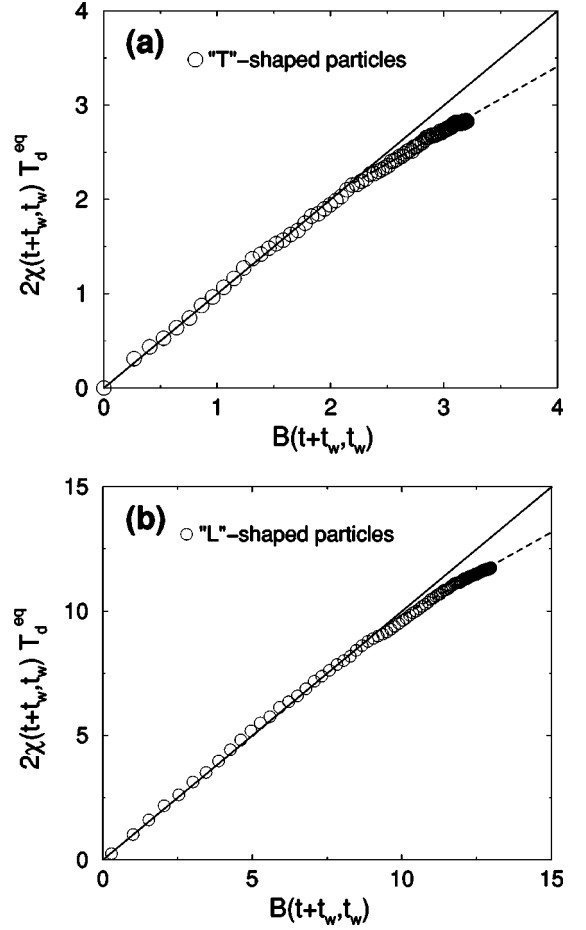

FIG. 5. Plot of the mobility $2T_d^{eq}\chi(t_w,t_w+t)$ vs the mean-square displacement $B(t_w,t_w+t)$ for different types of particles (with equal concentrations). (a) "T"-shaped particles and (b) "L"-shaped particles, $t_w=5\times10^4$. The dynamical temperatures associated with the two different types of particles (i.e., the slopes of the dashed straight lines) are equal to within the error bars.

easily, being less constrained. Although we have two different types of particles, the system remains homogeneous during compaction.

We have therefore measured FDR for the two different types of particles. The results obtained show that the two dynamical temperatures are equal within the error bars, even though the related diffusivities are different (see Fig. 5 for an example with equal fractions of T-shaped and L-shaped particles). This result has several important consequences. First of all the coincidence of the results for the dynamical temperature obtained with different observables is a crucial step for the establishment of a thermodynamical interpretation. Another important consequence arises from the experimental point of view: since the value of FDR is independent of the shape of the particles, it could be possible to measure the dynamical temperature of a granular material using a tracer particle different from the particles composing the system. This dynamical temperature should not depend on the shape of the tracer particle. The extension of this result to the case of compaction with gravity will be discussed in the following section.
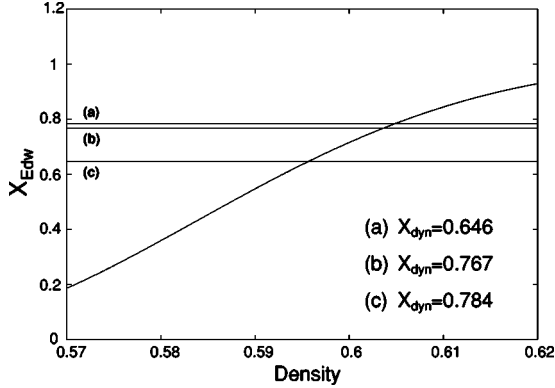
FIG. 6. Static ratio X_{Edw} as a function of density. The horizontal lines correspond to the dynamical ratios X_{dyn} measured at $t_w = 10^4$, 3×10^4, and 10^5 and determine the values $\rho_1 \approx 0.596$, $\rho_2 \approx 0.603$, and $\rho_3 \approx 0.605$, to be compared with Fig. 7.

E. Comparison with Edwards' measure

We are now in a position to compare the results for the fluctuation-dissipation ratio $X_{dyn} = T_d^{eq}/T_{dyn}$, measured during the compaction dynamics, with the outcomes of Edwards' approach at the corresponding densities. In Fig. 6 we report the values of X_{Edw} vs ρ (as obtained with the Edwards' measure) and X_{dyn} (obtained by the FDR in dynamical measurements) at three different values of t_w. In order to check the matching between X_{Edw} and X_{dyn} it is enough to compare the densities obtained from Fig. 6 by imposing $X_{Edw} = X_{dyn}$ with the corresponding dynamical densities obtained at the corresponding t_w. From Fig. 6 one gets: $\rho_1 \approx 0.596$ for $t_w^1 = 10^4$, $\rho_2 \approx 0.603$ for $t_w^2 = 3 \times 10^4$, $\rho_3 \approx 0.605$ for $t_w^3 = 5 \times 10^4$. On the other hand, the evolution of the density of the system during the measurements of the FDR is reported in Fig. 7. Since the measurements are performed *during* the compaction, the density is evolving, going from $\rho(t_w)$ to $\rho(t_w + t_{max})$. In each case, we obtain that indeed $\rho_i \in [\rho(t_w^i), \rho(t_w^i + t_{max})]$, where we have denoted with ρ_i the
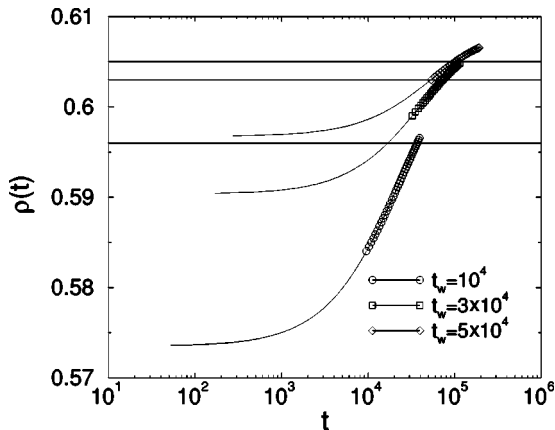

FIG. 7. Evolution of the density during the measurements of χ and B for $t_w = 10^4$, 3×10^4, and 10^5. The evolution during the quasiequilibrium part is plotted with lines, and during the violation of FDT with symbols. The horizontal lines correspond to the densities ρ_1, ρ_2, and ρ_3 from Fig. 6.

densities obtained from Fig. 6 for different values of t_w^i ($i = 1,2,3$). More precisely, ρ_i is very close to $\rho(t_w^i + t_{max})$. This is to be expected since the measure of the FDT violation is made for times much larger than t_w^i and, since the compaction is logarithmic, the system actually spends more time at densities close to $\rho(t_w^i + t_{max})$ than to $\rho(t_w^i)$.

V. FLUCTUATION-DISSIPATION RATIO FOR THE CASE WITH GRAVITY

A. Compaction dynamics

While the use of a compaction without gravity is useful to study an idealized context, real compaction due to shaking occurs because of gravity.

The standard way of simulating the effect of gravity in a lattice model is to let the particles diffuse on a tilted (square or cubic) lattice, with probabilities p_{up} ($p_{down} = 1 - p_{up}$) to go up (down), respecting the geometrical or kinetic constraints. A closed boundary is situated at the bottom of the simulation box, of horizontal linear size L and vertical size $L_z \gg L$ (lateral boundary conditions can be closed or open, and various aspect ratios can be used, without changing the results qualitatively). The control parameter is the ratio $x = p_{up}/p_{down} < 1$.

This corresponds, in fact, to the dynamics at temperature $T = -1/\ln(x)$ for the Hamiltonian

$$H = \sum_i z_i, \tag{6}$$

where the z_i are the heights of the particles (of either of the models under consideration) above the bottom. Indeed, attempted diffusion moves which respect the constraints are accepted with probability $\min(1, x^{\Delta H})$.

As a result, particles tend to diffuse more easily towards the bottom. A nonzero value of x is, however, needed in order to allow for rearrangements.

A simple lattice gas (with the only constraint of single occupancy) diffusing with the above rule displays an equilibrium behavior, with the known density profile

$$\rho(z) = \frac{1}{1 + \exp[\beta(z - z_0)]}, \tag{7}$$

(with $\beta = 1/T$ and z_0 depends on the number of particles) and time translation invariance, and FDT is obeyed. The system is therefore stationary and no evolution of the density occurs.

On the other hand, systems of constrained particles like the tetris or Kob-Andersen models are unable to reach this stationary state and are stuck at lower densities (larger potential energies), with slow compaction and aging, reproducing the phenomenology of granular compaction [8,11,21,35]. In particular, it has been shown, both experimentally and numerically, that, due to heterogeneities, the value of the potential energy (or of the bulk density) is not the only relevant parameter [10,11], and that, in order to explain for instance memory phenomenon, it is necessary to take into account the whole density profile along the vertical direction. For example, various density profiles can be obtained at ap-
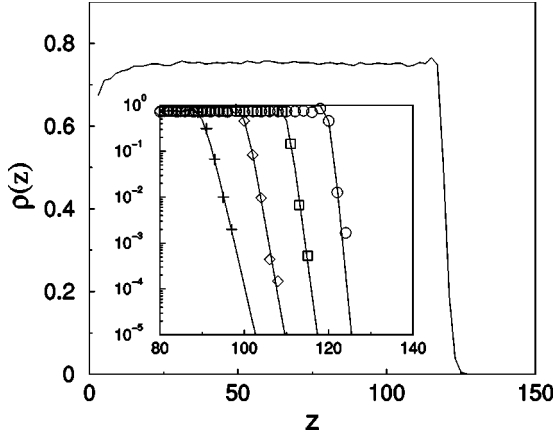
FIG. 8. Typical density profile obtained during the compaction dynamics of the KA model. The inset shows the dynamical interface for $x=0.1$ (circles), $x=0.2$ (squares), $x=0.3$ (diamonds), and $x=0.4$ (crosses) together with equilibrium interfaces of a lattice gas without constraints under gravity at the same shaking amplitudes (lines). The interface profiles have been horizontally shifted for clarity.

proximately the same potential energy, by varying the evolution of the forcing T with time.

A first order treatment consists in separating a slowly compacting bulk part and an interface [8]. Because the interface is much more dilute than the bulk, the particles feel much less the constraints, and it turns out that the density profile at the interface is exactly the same as the density profile of a lattice gas without constraints (see the inset of Fig. 8), with Hamiltonian (6) and forcing T. This part of the system can therefore *a priori* be considered as "in equilibrium," i.e., its shape and dynamics are simply linked to the forcing.

At this level of treatment, the system is therefore considered to be homogeneous in the horizontal directions, and heterogeneities are taken into account only in the vertical direction.

Compaction data, under the effect of gravity, for various types of tetris model can be found in Refs. [8,11,21] and for the KA model in Ref. [35]. Although we have monitored the usual quantities describing the compaction, we will therefore not repeat this analysis, but concentrate on the violation of FDT during compaction, showing *en passant* that the few existing data can be misleading or misinterpreted.

The existence of heterogeneities along the vertical direction moreover leads to the following remarks.

While calculating the Edwards' measure, imposing only the potential energy of the system will lead to a unique density profile. Since the dynamical density profile depends on the history, it is already clear that specifying only the energy will not be sufficient to predict all dynamical observables.

Heterogeneities exist only along the vertical direction, so that observables along the vertical and horizontal directions should *a priori* be treated separately.

Dynamical measures can either be made over the whole system or restricted to the bulk. In the first case, the interface will obviously give an "equilibrium" contribution that may be much larger than the bulk contribution.

Our numerical results have been performed in the following conditions.

Tetris model: horizontal size $L=40$, number of particles $N_{part}=1600$, number of runs $N_{runs}=2000$.

Kob-Andersen model: horizontal size $L=20-40$, number of particles $N_{part}=30\,000-50\,000$, number of runs $N_{runs}=20-50$.

B. FDT and its violations in the existence of a preferred direction

In general, the fluctuation-dissipation theorem relates, for a system at equilibrium, conjugated response and correlation functions:

$$TR(t,t') = \frac{\partial C(t,t')}{\partial t'}.$$

Integrated between t_w and $t+t_w$ in order to use the integrated response function, the relation becomes

$$T\chi(t+t_w,t_w) = C(t+t_w,t+t_w) - C(t+t_w,t_w). \quad (8)$$

Let us first consider the case of horizontal degrees of freedom: in these directions the system is homogeneous, and without drift. Then if we define

$$C_h(t+t_w,t_w) = \frac{1}{2N} \sum_{a=x,y} \sum_{i=1}^{N} \langle a_i(t_w+t)a_i(t_w)\rangle$$

$$-\frac{1}{2} \sum_{a=x,y} \left\langle \frac{1}{N}\sum_{i=1}^{N} a_i(t_w)\right\rangle$$

$$\times \left\langle \frac{1}{N}\sum_{i=1}^{N} a_i(t_w+t)\right\rangle \quad (9)$$

and

$$B_h(t+t_w,t_w) = \frac{1}{2N}\sum_{a=x,y}\sum_{i=1}^{N} \langle [a_i(t_w+t)-a_i(t_w)]^2\rangle, \quad (10)$$

it is easily seen that $B_h(t+t_w,t_w) = 2[C_h(t+t_w,t+t_w) - C_h(t+t_w,t_w)]$.

Moreover, to measure susceptibilities, a perturbation is applied in the following way: until t_w, the system evolves with forcing x and Hamiltonian (6); at t_w, a copy is made and evolves after t_w according to the perturbed Hamiltonian $H_\epsilon = \Sigma_i z_i^r + H_\epsilon^h$ where $H_\epsilon^h = \epsilon\Sigma_i(f_ix_i^r + g_iy_i^r)$, with $f_i,g_i = \pm 1$ randomly for each particle and x_i^r,y_i^r,z_i^r are the positions of the particles in the perturbed system. The integrated response

$$\chi_h(t_w+t,t_w) = \frac{1}{2\epsilon N}\sum_{i=1}^{N} \langle \overline{f_i[x_i^r(t_w+t)-x_i(t_w)]} + \overline{g_i[y_i^r(t_w+t)-y_i(t_w)]}\rangle \quad (11)$$

can then be measured.

For a system at equilibrium [for example, the simple lattice gas with single occupancy and no kinetic constraints, and Hamiltonian (6)], the FDT relation can be observed,

$$B_h(t_w+t,t_w)=2T\chi_h(t_w+t,t_w). \tag{12}$$

During compaction, the violation of FDT can then be investigated from a parametric plot of χ_h vs B_h. This is exactly similar to the homogeneous case of Sec. IV.

Up to now, however, the only tentative measures of FDR have been realized with observables coupled to the vertical direction [30,31]. This is in contrast with other cases of systems with a preferential direction, where measures along the only direction with no *a priori* heterogeneities were undertaken [29,41,42].

In Ref. [31], the case of the KA model with a vertical random perturbation was considered. The vertical mean-square displacement

$$B_v(t+t_w,t_w)=\frac{1}{N}\sum_{i=1}^{N}\left\langle[z_i(t_w+t)-z_i(t_w)]^2\right\rangle$$

was measured and confronted to the integrated response

$$\chi_v(t_w+t,t_w)=\frac{1}{\epsilon N}\sum_{i=1}^{N}\overline{\left\langle f_i[z_i^r(t_w+t)-z_i(t_w)]\right\rangle}$$

to a perturbation $H_\epsilon^v=\epsilon\Sigma_i f_i z_i^r$ ($f_i=\pm1$ randomly). The existence of a dynamical temperature was inferred from the observed linear relation between B_v and χ_v, with a slope different from the applied temperature.

In Ref. [30], a perturbation in the forcing was applied, and confronted to the following mean-square displacement:

$$\widetilde{B}_v(t+t_w,t_w)=\left\langle[h(t_w+t)-h(t_w)]^2\right\rangle$$

with $h(t)=\Sigma_i z_i(t)/N$. The perturbation in the forcing leads to the observation of negative response functions [$\widetilde{\chi}_v(t+t_w,t_w)=h^r(t+t_w)-h(t+t_w)$, where h^r is the mean height of the perturbed system, the perturbation being applied after t_w], interpreted as the signature of a "negative dynamical temperature." This case was investigated in Refs. [8,11] where this result was shown to be linked to the existence of memory effects, as also confirmed in experiments [10].

In both cases, however, the existence of a downward drift, due to compaction, was not taken into account for the correct definition of the correlation part of the fluctuation-dissipation relation: indeed, in the first case, the correlation being

$$C_v(t+t_w,t_w)=\frac{1}{N}\sum_{i=1}^{N}\left\langle z_i(t_w+t)z_i(t_w)\right\rangle-\left\langle\frac{1}{N}\sum_{i=1}^{N}z_i(t_w)\right\rangle$$

$$\times\left\langle\frac{1}{N}\sum_{i=1}^{N}z_i(t_w+t)\right\rangle, \tag{13}$$

$B_v(t+t_w,t_w)$ is not proportional to $C_v(t+t_w,t+t_w)-C_v(t+t_w,t_w)$ as in the homogeneous case. This is even more easily seen in the second case, where the correlation conjugated to the response to a change in the driving is $\widetilde{C}_v(t+t_w,t_w)=\left\langle h(t+t_w)h(t_w)\right\rangle-\left\langle h(t+t_w)\right\rangle\left\langle h(t_w)\right\rangle$. Indeed

$$\widetilde{B}_v(t+t_w,t_w)=\left\langle h^2(t+t_w)+h^2(t_w)\right\rangle-2\left\langle h(t+t_w)h(t_w)\right\rangle$$

and

$$\widetilde{C}_v(t+t_w,t+t_w)-\widetilde{C}_v(t+t_w,t_w)=\left\langle h^2(t+t_w)\right\rangle$$
$$-\left\langle h(t+t_w)h(t_w)\right\rangle-\left\langle h(t+t_w)\right\rangle\left\langle h(t+t_w)-h(t_w)\right\rangle \tag{14}$$

are not simply related since $\left\langle h(t+t_w)\right\rangle\neq\left\langle h(t_w)\right\rangle$ and $\left\langle h^2(t+t_w)\right\rangle\neq\left\langle h^2(t_w)\right\rangle$ (see also a similar discussion, on the case of one-time quantities changing with time, in Ref. [43]).

It turns out therefore that the results of Refs. [30,31] are *a priori* flawed from an incorrect measure of the correlation part of FDR.

We will see in the next subsections how measures of correlation and response functions along the horizontal directions lead to sensible results, whereas all measures of vertical correlations or response lead to the impossibility of defining effective temperatures.

C. FDR in the aging (compacting) regime

1. Vertical observables?

Two sets of response and correlation functions can *a priori* be measured: the incoherent ones (C_v,χ_v) as in Ref. [31] or the coherent ones ($\widetilde{C}_v,\widetilde{\chi}_v$) as in Ref. [30].

If we write

$$C_v(t+t_w,t+t_w)-C_v(t+t_w,t_w)$$

$$=\left\langle\frac{1}{N}\sum_{i=1}^{N}z_i(t+t_w)[z_i(t+t_w)-z_i(t_w)]\right\rangle$$

$$+\frac{1}{N}\left\langle\sum_{i=1}^{N}z_i(t+t_w)\right\rangle\left\langle\frac{1}{N}\sum_{i=1}^{N}[z_i(t_w)-z_i(t+t_w)]\right\rangle$$

$$=\left\langle\frac{1}{N}\sum_{i=1}^{N}[z_i(t_w)-z_i(t+t_w)][\left\langle h(t+t_w)\right\rangle-z_i(t+t_w)]\right\rangle$$

we can observe that generically $z_i(t_w+t)\leq z_i(t_w)$ since the system is compacting, so that two opposite contributions can be distinguished in $C_v(t+t_w,t+t_w)-C_v(t+t_w,t_w)$: the particles such that $z_i(t+t_w)<h(t+t_w)$ give a positive contribution, those such that $z_i(t+t_w)>h(t+t_w)$ give a negative one. At short and intermediate times, the particles closer to the surface move more than those in the bulk and therefore the negative contribution dominates. This leads to a negative $C_v(t+t_w,t+t_w)-C_v(t+t_w,t_w)$. At very long times $C_v(t+t_w,t+t_w)-C_v(t+t_w,t_w)$ has to become positive by definition, but such times may not be reachable in a numerical simulation.

This peculiar behavior comes from the fact that the drift is not homogeneous in the system: some regions are compact-
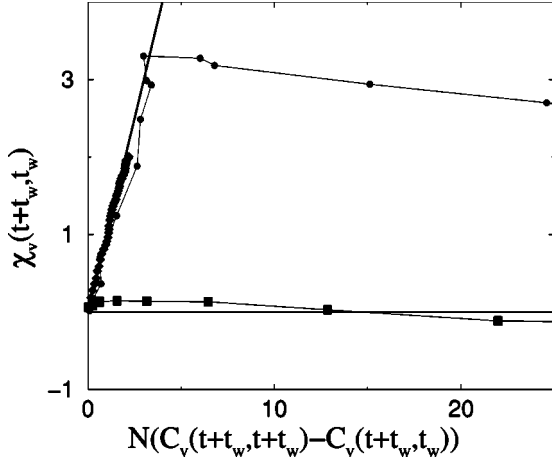
FIG. 9. $\tilde{\chi}_v(t+t_w,t_w)$ vs $N[\tilde{C}_v(t+t_w,t+t_w)-\tilde{C}_v(t+t_w,t_w)]$ for the KA model, with $L=20$, $N_{part}=4000$, $N_{run}=500$, $x=0.8$ (circles), and $x=0.5$ (squares); $t_w=2^{14}$ and $t=2,\ldots,2^{16}$. The first equilibrium part corresponds to the interface dynamics, while at longer times $\tilde{\chi}_v$ decreases because of the bulk response. The diamonds correspond to a simulation with no kinetic constraint and $N_{part}=4000$ particles: only equilibrium FDT is then observed. The straight line has slope 1.

ing more than others. Local drifts should then be taken into account. However, this is numerically (and also experimentally) too difficult to measure.

On the other hand, the coherent correlation and response $\tilde{C}_v$, $\tilde{\chi}_v$ can also be measured. The difficulty arises from the measure of the coherent correlation function $\tilde{C}_v$, of order $1/N$ for N particles: relatively small systems have to be simulated with a large number of realizations. For an equilibrium lattice gas without kinetic constraints, FDT is then recovered: $N[\tilde{C}_v(t+t_w,t+t_w)-\tilde{C}_v(t+t_w,t_w)]=\tilde{\chi}_v(t+t_w,t_w)$. In the case of the compacting system, the parametric plot of $N[\tilde{C}_v(t+t_w,t+t_w)-\tilde{C}_v(t+t_w,t_w)]$ vs $\tilde{\chi}_v(t+t_w,t_w)$ reveals a first part of slope one, which corresponds to the fast, equilibrium response of the interface. At larger times t, however, the response of the bulk, which can compactify more easily if the forcing is increased, leads to a decrease of $\tilde{\chi}_v(t+t_w,t_w)$, which can even become negative as observed in Ref. [30]. As t_w goes to ∞, the bulk becomes so compact that its contribution goes to zero, and the equilibrium FDT can be recovered thanks to the interface contribution. Those results are summarized in Fig. 9.

The previous investigations shows that no definition of an effective temperature can be inferred from dynamical measures correlated with the preferred directions in which heterogeneities occur.

Note that this kind of situation also arises in the study of effective temperatures in driven vortex lattices with random pinning: while an effective temperature can be defined and measured for degrees of freedom perpendicular to the drive, problems are encountered when dealing with longitudinal observables [44]. We now turn to horizontal observables.

2. Horizontal observables

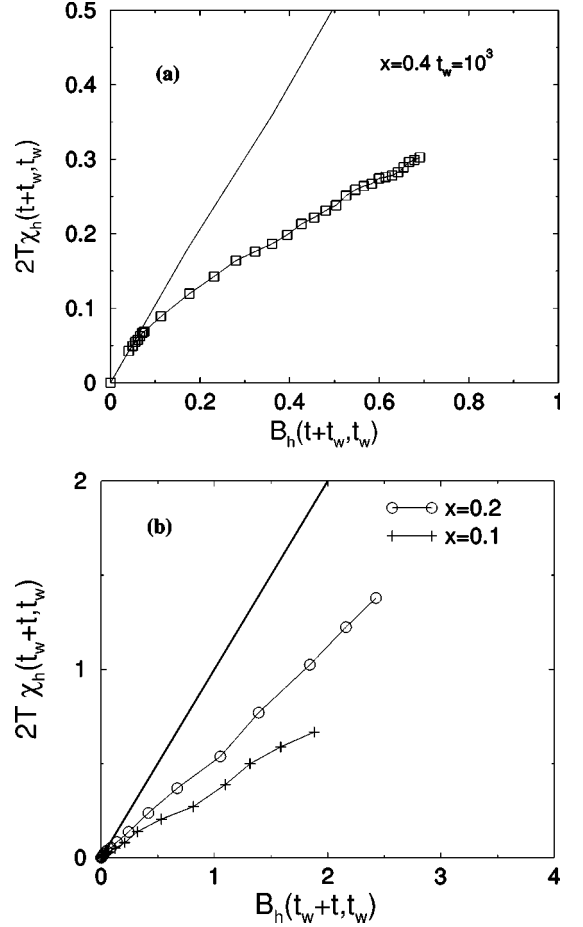The first result is obtained by studying the whole system with a horizontal perturbation applied: the relation between

FIG. 10. $2T\chi_h$ vs B_h for the tetris model (a) and the KA model ($t_w=2^{14}$)(b). The straight lines have slope 1.

mean-square displacement B_h and response function χ_h is then clearly linear, with a slope equal to the temperature T of the forcing. This seemingly surprising result is easily explained by the fact that both functions are completely dominated by the contribution of the interface where the particles can diffuse quite easily, and which actually displays an equilibrium profile (see Fig. 8). It seems therefore natural to restrict the study of the observables to the bulk part of the sample, in which the density is quite homogeneous when a constant forcing is applied (see Refs. [11,35] and Fig. 8). The sums defining B_h, χ_h are therefore restricted to the particles that remain between t_w and t_w+t in the bulk (defined, e.g., as $z_{min}<z_i<z_{max}$, with z_{min} and z_{max} appropriately chosen).

Our results, summarized in Fig. 9 and 10, are qualitatively similar for both models. The clear violation of FDT obtained with horizontal perturbations allows for the measurements of the FD ratios while nothing can be said using the data obtained with vertical perturbations.

D. Results for a bidisperse system

In the models we have considered, it is quite easy to implement the presence of two types of particles (this has already been seen in Sec. IV for the tetris model without gravity).
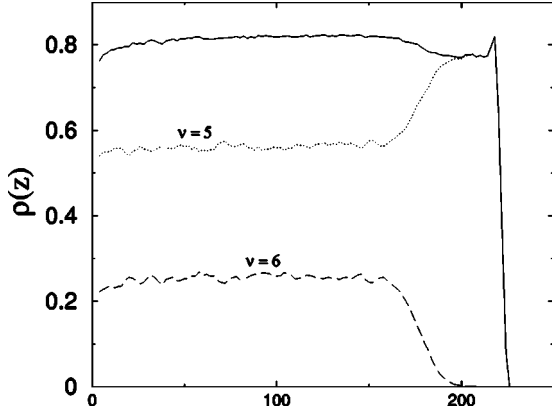
FIG. 11. Density profiles for a bidisperse system of 30 000 particles with $\nu_1 = 5$ and 10 000 particles with $\nu_2 = 6$, for a forcing $x = 0.2$, after 2^{14} time steps. The less constrained particles have diffused more easily towards the bottom.

For the Kob-Andersen model, we can simulate "small" and "large" particles by taking different values for the kinetic constraint, e.g., $\nu_1 = 5$ and $\nu_2 = 6$ or $\nu_2 = 7$. As also shown in Ref. [35], partial segregation then occurs because the particle with larger ν are less constrained and can move more easily toward the bottom.

However, as shown in Fig. 11, there exists a bulk region in which the density profiles for both types of particles are flat. It is therefore possible to measure FDR in this region.

The results, shown in Fig. 12, are quite clear: although the smaller particles are more mobile than the larger ones, and therefore diffuse more easily, the FDR for the two types of particles are equal. As already noted in Sec. IV, this result is important since it means that the FDR can in principle be measured using tracers different from the particles compos-
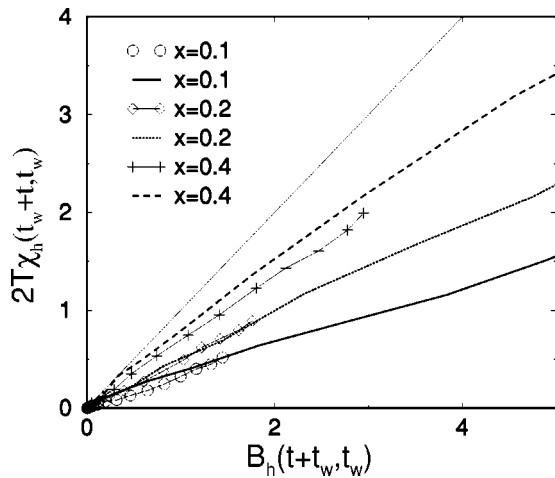

FIG. 12. KA model: $2T\chi_h$ vs B_h, measured in the homogeneous bulk, for the two types of particles (symbols, more constrained particles with $\nu_1 = 5$; lines, less constrained particles with $\nu_2 = 6$), for various forcing (0.1, 0.2, and 0.4) and $t_w = 2^{14}$, $t = 2, \ldots, 2^{18}$. The two kinds of particles display different χ_h and B_h at a given time, but the same violation of FDT.
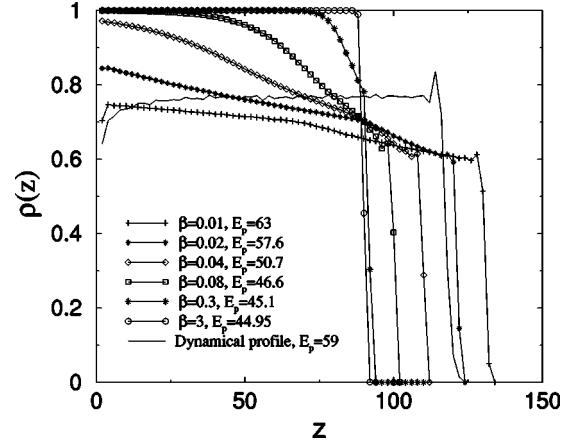

FIG. 13. KA model: density profiles for Edwards' measure, obtained with various values of the Lagrange parameter β (symbols). A dynamically obtained profile is also shown for comparison, it corresponds to a constant shaking $x = 0.4$ and to a potential energy similar to the case $\beta = 0.02$ (stars). The profiles are very different.

ing the granular material, and that the FDR should then be independent of the shape of the tracer.

E. Edwards' measure

Edwards' measure is defined as a flat measure over all blocked configurations, i.e., configurations with all particles unable to move. For a system under gravity, a particle at height z is "blocked" if it cannot move downwards, i.e. if all its neighboring sites at $z - 1$ are occupied or if the particle cannot move towards either of these sites because of the geometrical or kinetic constraints.

Implementing this difference (with respect to the case without gravity) into the auxiliary model of Refs. [23,24] is straightforward.

As in Ref. [29], the following procedure is used: the auxiliary model has total "energy" $\beta_{aux}E_{aux} + \beta E_p$ where E_{aux} is as usual the number of mobile particles, β_{aux} the auxiliary inverse temperature, E_p the potential energy, and β a Lagrange multiplier. For each value of β, an annealing procedure is performed on β_{aux}, until configurations with $E_{aux} = 0$ are reached. The density profiles are then measured, along with the value of E_p. Repeating the procedure then yields the curve $\beta_{Edw}(E_p)$ directly. The profiles at various values of E_p are shown in Fig. 13. These profiles are quite different from the dynamically obtained profiles at similar energies. This is not surprising since they have been obtained imposing only the potential energy, whereas the dynamical profiles depend on the history and it has been shown [8,10,11] that E_p is not the only relevant parameter.

In this case, Edwards' measure, if constructed by imposing only one parameter, is not able to predict dynamical observables.

On the other hand, since dynamically the bulk density profiles are flat, we can generate blocked configurations with homogeneous density, at various densities. This yields a restricted Edwards' measure; proceeding as in Refs. [23,24] we obtain Edwards' entropy at the densities considered and we can therefore compute
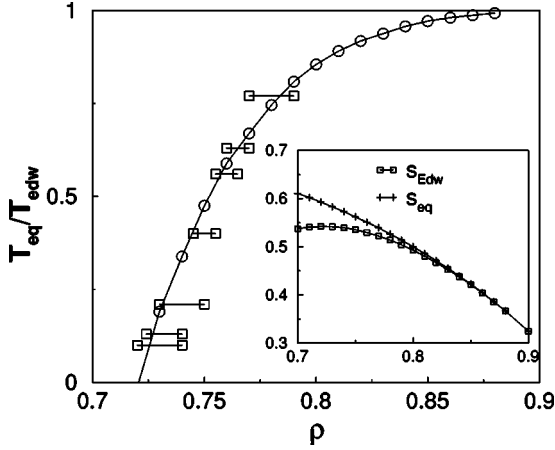
FIG. 14. Circles, $X_{Edw}=(ds_{equil}(\rho)/d\rho)/(ds_{Edw}(\rho)/d\rho)$ vs ρ for KA model, imposing homogeneity; squares, dynamically obtained FDR (for horizontal displacements and response) vs density measured for the corresponding dynamical profiles. Inset, equilibrium and Edwards' entropy densities (imposing homogeneity for Edwards' entropy).

$$X_{Edw}=\frac{\dfrac{ds_{equil}(\rho)}{d\rho}}{\dfrac{ds_{Edw}(\rho)}{d\rho}}, \qquad (15)$$

which is shown in Fig. 14 in the case of the KA model.

F. Comparison and discussion

From the dynamics on the one hand and Edwards' measure on the other hand the following two sets of data are obtained.

Dynamical FDR at various densities, for horizontal displacements and response functions; since the density is evolving during the measures, an uncertainty is observed.

Statically obtained X_{Edw}.

Figure 14 shows that the agreement between both sets of data is very good, even for a quite large vibration $x=0.4$ or low densities 0.73.

The theoretical results can be summarized as follows: in the case of a homogeneous bulk, the ratio X_d of the horizontal dynamical temperature to the imposed temperature $-1/\ln(x)$ only depends on the bulk density, and is given by $X_{Edw}(\rho)$. Using various vibration amplitudes, we have checked that X_d at various densities and $X_{Edw}(\rho)$ indeed coincide. Another check of the consistency of the theoretical construction can be made by comparing two dynamical procedures: if a certain forcing T_1 is applied until t_w, and then changed to T_2, a dynamical temperature T_d^{12} will be obtained. While T_d^{12} depends on T_2, the equality

$$\frac{T_2}{T_d^{12}}=X_{Edw}[\rho(t_w)]$$

should be observed, at least if T_2 is not much higher than T_1 (in this case, as shown in Ref. [11], the bulk density changes
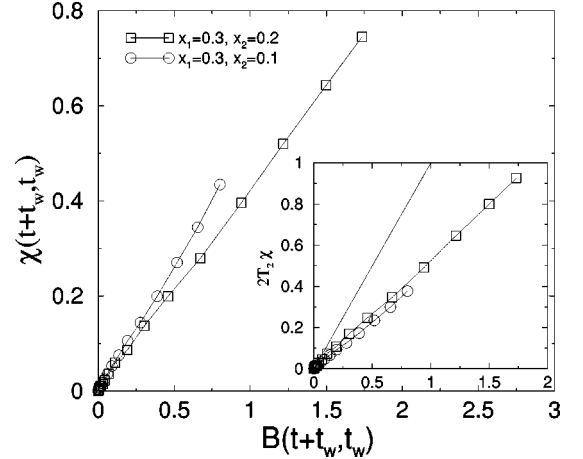

FIG. 15. χ vs B following a change in the forcing from x_1 to x_2 at $t_w=2^{14}$: the slope depends on the forcing applied after t_w ($t=2,\ldots,2^{18}$). Inset, $T_2\chi$ vs B, showing the equality of the dynamical ratios T_2/T_{dyn}.

suddenly by a large amount after t_w). We have performed such measurements and checked that this is indeed the case (see Fig. 15).

VI. RELATIONS WITH EXPERIMENTS

While the link between a dynamically measured temperature and a static measure is of great theoretical importance, it is experimentally impossible to sample such a measure. Theoretical predictions can be checked experimentally only through purely dynamical measures.

Preliminary results in this direction were obtained by the Chicago group [4] by measuring the volume fluctuations with respect to the steady-state volume at different heights of the sample. Since the curves obtained at different heights do not coincide, the authors concluded that one single observable, namely, the Edwards compactivity, cannot account for the depth dependence of the fluctuations. These conclusions are in agreement with our results obtained in systems with a preferential direction where fixing one single observable in the Edwards approach does not allow for the prediction of the dynamical observables unless one reduces the analysis to some homogeneous section of the system.

Thanks to recent theoretical progresses, new experiments have been proposed in order to check the existence of dynamical temperatures [23,29,41,42], by monitoring mean-square displacements and mobility of tagged particles, or tracers, in sheared supercooled liquids or foams, or in sheared or tapped granular media. The existence of a linear relation (B vs χ) could be tested for various shapes, masses, etc., of the tracers, in order to check that this relation is indeed defining a temperature.

Our analysis of models compacting under gravity suggests also other types of experimental possibilities. First, only diffusivity and mobility in the direction perpendicular to the gravity should be measured. Moreover, the existence of strong heterogeneities implies that a tracer close to the interface should allow to measure a temperature T_d^i which de-

pends directly on the driving amplitude [in the models, $T = -1/\ln(x)$], and is stationary, i.e., does not depend on the bulk density. On the other hand, a tracer well immersed in the bulk should yield another value T_d^b of the FDR (which depends on t_w), and the *ratio* T_d^b/T_d^i should depend only on the density of the bulk. For example, if experiments are performed changing the driving intensity at t_w from x_1 to x_2, and the two associated ''interface'' and ''bulk'' temperatures are measured, the ratio T_d^b/T_d^i should be independent of x_2, provided the bulk density does not change significantly. In this way, the comparison of only dynamical measures would be a strong experimental test for the whole theoretical construction, without any need to sample the underlying static measure.

VII. SUMMARY AND CONCLUSIONS

In this paper, we have studied two paradigmatic models for the compaction of granular media. These models consider particles diffusing on a lattice, with either geometrical or dynamical constraints. Idealized compaction without gravity has been implemented for the tetris model, and compaction with a preferential direction imposed by gravity has been studied for both models. The possibility to define dynamically a temperature in the framework of fluctuation-dissipation relations and to link it to the statically constructed Edwards' measure has been investigated.

In the first, ideal, case of the homogeneous compaction, the obtained FD ratios have been clearly shown to be in agreement with the prediction of Edwards' measure at various densities.

The situation is more complicated if a preferential direction is present: then the whole density profile has *a priori* to be taken into account. Moreover, the vertical drift due to compaction leads to contradictory (and sometimes meaningless) results when observables coupled to the preferential direction are considered for the evaluation of a FD ratio [30,31]. Since the energy of the system is not the only parameter, and since the density profiles depend on the history, Edwards' measure is not *a priori* able to predict the dynamical configurations. If, however, the homogeneity of the bulk is imposed, FD ratio obtained dynamically for horizontal displacements and mobility and from Edwards' measure coincide.

It is striking to note that Edwards' measure, which *a priori* could be valid only for very weak forcing and almost stationary systems seems, however, to yield good predictions even for nonstationary systems that are still compacting.

Finally, we have proposed experimental tests of the whole theoretical construction, through the comparison of various types of dynamical measurements, since the construction of Edwards' measure, numerically straightforward, is obviously impossible in experiments.

[1] H.M. Jaeger and S.R. Nagel, Science **255**, 1523 (1992).

[2] H.M. Jaeger, S.R. Nagel, and R.P. Behringer, Rev. Mod. Phys. **68**, 1259 (1996).

[3] For a recent introduction to the overall phenomenology, see *Physics of Dry Granular Media*, edited by H. J. Herrmann and S. Luding (Kluwer Academic, Dordrecht, 1998), pp. 553–583.

[4] J.B. Knight, C.G. Fandrich, C.N. Lau, H.M. Jaeger, and S.R. Nagel, Phys. Rev. E **51**, 3957 (1995); E.R. Nowak, J.B. Knight, M. Povinelli, H.M. Jaeger, and S.R. Nagel, Powder Technol. **94**, 79 (1997); E.R. Nowak, J.B. Knight, E. Ben-Naim, H.M. Jaeger, and S.R. Nagel, Phys. Rev. E **57**, 1971 (1998); H.M. Jaeger, in *Physics of Dry Granular Media* (Ref. [3]), pp. 553–583.

[5] P. Philippe and D. Bideau (unpublished).

[6] M. Nicolas, P. Duru, and O. Pouliquen, Eur. Phys. J. E **3**, 309 (2000).

[7] M. Nicodemi and A. Coniglio, Phys. Rev. Lett. **82**, 916 (1999).

[8] A. Barrat and V. Loreto, J. Phys. A **33**, 4401 (2000).

[9] J. Talbot, G. Tarjus, and P. Viot, Eur. Phys. J. E **5**, 445 (2001).

[10] C. Josserand, A. Tkachenko, D.M. Mueth, and H.M. Jaeger, Phys. Rev. Lett. **85**, 3632 (2000).

[11] A. Barrat and V. Loreto, Europhys. Lett. **53**, 297 (2001).

[12] J.J. Brey and A. Prados, J. Phys.: Condens. Matter **14**, 1489 (2002).

[13] H.J. Herrmann, J. Phys. II **3**, 427 (1993).

[14] G.C. Barker and A. Mehta, Phys. Rev. E **47**, 184 (1993).

[15] M. Nicodemi, A. Coniglio, and H.J. Herrmann, Phys. Rev. E **59**, 6830 (1999).

[16] E. Ben-Naim, J.B. Knight, and E.R. Nowak, Physica D **123**, 380 (1998); P.L. Krapivsky and E. Ben-Naim, J. Chem. Phys. **100**, 6778 (1994).

[17] T. Boutreux and P.G. de Gennes, Physica A **244**, 59 (1997).

[18] S.F. Edwards, in *Granular Matter: An Interdisciplinary Approach*, edited by A. Mehta (Springer-Verlag, New York, 1994), and references therein; S.F. Edwards, J. Stat. Phys. **62**, 889 (1991); A. Mehta and S.F. Edwards, Physica A **157**, 1091 (1989).

[19] A. Mehta, R.J. Needs, and S. Dattagupta, J. Stat. Phys. **68**, 1131 (1992).

[20] L.C.E. Struik, *Physical Ageing in Amorphous Polymers and Other Materials* (Elsevier, Houston, 1978).

[21] E. Caglioti, V. Loreto, H.J. Herrmann, and M. Nicodemi, Phys. Rev. Lett. **79**, 1575 (1997).

[22] E. Caglioti and V. Loreto, Phys. Rev. Lett. **83**, 4333 (1999).

[23] A. Barrat, J. Kurchan, V. Loreto, and M. Sellitto, Phys. Rev. Lett. **85**, 5034 (2000).

[24] A. Barrat, J. Kurchan, V. Loreto, and M. Sellitto, Phys. Rev. E **63**, 051301 (2001).

[25] W. Kob and H.C. Andersen, Phys. Rev. E **48**, 4364 (1993).

[26] V. Colizza, V. Loreto, and A. Barrat, Phys. Rev. E **65**, 050301 (2002).

[27] J. Brey, A. Prados, and B. Sanchez-Rey, Phys. Rev. E **60**, 5685 (1999); Physica A **275**, 310 (2000).

[28] A. Lefèvre and D.S. Dean, J. Phys. A **34**, L213 (2001); Phys. Rev. E **64**, 046110 (2001).

[29] H. Makse and J. Kurchan, Nature (London) **415**, 614 (2002).

[30] M. Nicodemi, Phys. Rev. Lett. **82**, 3734 (1999).

[31] M. Sellitto, Phys. Rev. E **63**, 060301 (2001).

[32] For a review, see, W. Götze, in *Liquids, Freezing and Glass Transition*, J.P. Hansen, D. Levesque, and J. Zinn-Justin (North Holland, Amsterdam, 1989).

[33] J. Kurchan, L. Peliti, and M. Sellitto, Europhys. Lett. **39**, 365 (1997).

[34] M. Sellitto, Eur. J. Phys. **4**, 135 (1998).

[35] M. Sellitto and J.J. Arenzon, Phys. Rev. E **62**, 7793 (2000).

[36] A. Bortz, M.H. Kalos, and J.L. Lebowitz, J. Comput. Phys. **17**, 10 (1975).

[37] L.F. Cugliandolo and J. Kurchan, Phys. Rev. Lett. **71**, 173 (1993); J. Phys. A **27**, 5749 (1994).

[38] G. Parisi, Phys. Rev. Lett. **79**, 3660 (1997).

[39] W. Kob and J.L. Barrat, Europhys. Lett. **46**, 637 (1999).

[40] L.F. Cugliandolo, J. Kurchan, and L. Peliti, Phys. Rev. E **55**, 3898 (1997).

[41] I.K. Ono, C.S. O'Hern, S.A. Langer, A.J. Liu, and S.R. Nagel, e-print cond-mat/0110276.

[42] L. Berthier and J.L. Barrat, e-print cond-mat/0110257; J. Chem. Phys. **116**, 6228 (2002).

[43] A. Buhot and J.P. Garrahan, Phys. Rev. Lett. **88**, 225702 (2002).

[44] L. Cugliandolo (private communication).

[45] We will see in Sec. V that the situation is, however, more complex and that great care has to be taken when measuring FDT violations under gravity.